

Topological nodal Cooper pairing in doped Weyl metals

Yi Li¹ and F. D. M. Haldane²

¹*Princeton Center for Theoretical Science, Princeton University, Princeton, NJ 08544, USA*

²*Department of Physics, Princeton University, Princeton, NJ 08544, USA*

(Dated: October 11, 2015)

We generalize the concept of Berry connection of the single-electron band structure to the two-particle Cooper pair states between two Fermi surfaces with opposite Chern numbers. Because of underlying Fermi surface topology, the pairing Berry phase acquires non-trivial monopole structure. Consequently, pairing gap functions have the topologically-protected nodal structure as vortices in the momentum space with the total vorticity solely determined by the monopole charge q_p . The pairing nodes behave as the Weyl-Majorana points of the Bogoliubov-de Gennes pairing Hamiltonian. Their relation with the connection patterns of the surface modes from the Weyl band structure and the Majorana surface modes inside the pairing gap is also discussed. Under the approximation of spherical Fermi surfaces, the pairing symmetry are represented by monopole harmonic functions. The lowest possible pairing channel carries angular momentum number $j = |q_p|$, and the corresponding gap functions are holomorphic or anti-holomorphic functions on Fermi surfaces.

PACS numbers: 74.20.Rp, 73.43.-f, 03.65.Vf

The study of topological states has renewed our understanding of condensed matter physics. The discovery of two-dimensional integer quantum Hall states^{1,2} initiated the exploration of novel states characterized by band topology rather than symmetry³⁻⁸, with magnetic band structures that possess non-trivial Chern numbers arising from broken time-reversal (TR) symmetry. The study of Berry curvature of Bloch bands in such lattice structures has led to many results in anomalous Hall and quantum anomalous Hall physics⁹⁻¹⁶. The band structure topology has also been generalized to systems of topological insulators with TR symmetry¹⁷⁻²⁷. The stable gapless surface modes which appear at the boundary of gapped topological systems have analogs in gapless semi-metallic systems, which can also have non-trivial band topology. For example, topological Weyl semi-metals have been proposed and realized in three-dimensional (3D) systems in the absence of either TR or inversion symmetry²⁸⁻⁵⁵. Their band structure is characterized by degenerate Weyl points in the Brillouin-zone (BZ), which can be understood as monopole sources and sinks of Berry-curvature flux in \mathbf{k} -space.

Topological phenomena are usually understood in terms of contributions from all the filled electronic states rather than the states in the vicinity of Fermi surfaces. The apparent disagreement with the central tenet of Fermi-liquid theory that all conduction processes can be understood at the Fermi level can be resolved by introducing the Berry phase of quasiparticles on the Fermi surface¹³. So far, the study of the Fermi surface topology and the associated Berry phase structure has mainly been discussed at the single-particle level¹¹⁻¹⁴.

Here we study a novel class of exotic superconductivity which can be realized in doped Weyl metals, and more generally in systems with topologically non-trivial Fermi surfaces. In superconductivity with pairing between states on two disjoint Fermi surface sheets with opposite Chern numbers, the Cooper pair inherits a non-

trivial Berry structure from the underlying single-particle Fermi surfaces. Consequently, the pairing gap functions develop nontrivial net vorticities leading to topologically-stable gapless nodes on the Fermi surfaces. These nodes also determine the interplay between the surface modes due to the Weyl point of the band structure and those arising from the Cooper pairing. For Fermi surfaces with approximate spherical symmetries, the pairing symmetry can be classified by the monopole harmonic functions rather than ordinary spherical harmonic functions.

We consider a general 3D electron system with a pair of separated Fermi surfaces, denoted as FS_\pm , respectively, carrying opposite Chern numbers $\pm C$. The doped Weyl metal can be thought as a concrete example. Let us start with a minimal description that only assumes the existence of parity (inversion) symmetry but broken TR symmetry. In this model, there are two Weyl points located at $\pm \mathbf{K}_0$, and are related to each other by parity (inversion) and respectively surrounded by FS_\pm . Furthermore, the parity ensures that opposite monopole charges $\pm q$ are enclosed by FS_\pm . Define the electron creation operator $c_a^\dagger(\mathbf{k})$ in which a is the index of a general two-band structure. For the single-electron states on FS_\pm , their creation operators are defined, respectively, as $\alpha_\pm^\dagger(\pm \mathbf{k}) = \sum_a \xi_{\pm,a}(\pm \mathbf{k}) c_a^\dagger(\pm \mathbf{K}_0 \pm \mathbf{k})$, in which $\pm \mathbf{k}$ are the relative momenta for electrons on FS_\pm with respect to $\pm \mathbf{K}_0$. $\xi_{\pm,a}(\pm \mathbf{k})$ are the corresponding normalized eigen-functions on FS_\pm , respectively. And $\pm \mathbf{k}$ lie on two surfaces denoted as S_\pm which correspond to shifting FS_\pm by $\mp \mathbf{K}_0$ towards the origin. Because of the non-trivial monopole structure, $\xi_{\pm,a}(\pm \mathbf{k})$ cannot be globally well-defined for $\pm \mathbf{k}$ over the entire surfaces of S_\pm , respectively. They need to be described using a specific gauge.

The single-particle Berry connection can be defined as $\mathbf{A}_\pm(\mathbf{k}) = \sum_a \xi_{\pm,a}^*(\mathbf{k}) i \nabla_{\mathbf{k}} \xi_{\pm,a}(\mathbf{k})$, in which $\nabla_{\mathbf{k}}$ lies in the tangent space of S_\pm , and, \mathbf{A}_\pm is a tangent vector field therein. The Berry fluxes satisfy $\iint_{S_\pm} d\mathbf{k} \cdot \nabla_{\mathbf{k}} \times \mathbf{A}_\pm(\mathbf{k}) = \pm 4\pi q$. The simplest case of $C = 1$ is associated with the

arXiv:1510.01730v2 [cond-mat.str-el] 12 Oct 2015

fundamental monopole charge of $q = \frac{1}{2}$.

Let us consider the zero-momentum inter-Fermi surface pairing between FS_+ and FS_- . The pairing operator $P^\dagger(\mathbf{k}) = \alpha_+^\dagger(\mathbf{k})\alpha_-^\dagger(-\mathbf{k})$. The Berry connection of the two-particle state created by $P^\dagger(\mathbf{k})$ is calculated as $\mathbf{A}_p(\mathbf{k}) = \mathbf{A}_+(\mathbf{k}) - \mathbf{A}_-(-\mathbf{k})$. The total pairing Berry flux penetrating S_+ is $\iint_{S_+} d\mathbf{k} \cdot \nabla_{\mathbf{k}} \times \mathbf{A}_p(\mathbf{k}) = 4\pi q_p$ with $q_p = 2q$. In other words, the inter-Fermi surface Cooper pairing inherits the Berry fluxes of two single-electron Fermi surfaces. Consequently, the Cooper pairing phases cannot be well-defined over the entire Fermi surfaces, which leads to the following theorem.

Consider the gap function over S_+ as $\Delta(\mathbf{k})$, which is conjugate to the pairing operator $P^\dagger(\mathbf{k})$ and is a single-valued complex function. Assuming the nodal structure of $\Delta(\mathbf{k})$ only composed of isolated points or lines, we have

Theorem. $\Delta(\mathbf{k})$ possesses generic nodal structure with the total vorticity $2q_p$, which is a consequence of the band topology on FS_\pm and is independent of specific pairing mechanisms and symmetries.

Proof. The gap function $\Delta(\mathbf{k})$ can be parameterized as $|\Delta(\mathbf{k})|e^{i\phi(\mathbf{k})}$ in which $\phi(\mathbf{k})$ is the pairing phase. $\Delta(\mathbf{k})$ is gauge-covariant as follows: Under the gauge transformation $\xi_\pm(\pm\mathbf{k}) \rightarrow \xi_\pm(\pm\mathbf{k})e^{i\Lambda_\pm(\pm\mathbf{k})}$, we have $\alpha_\pm^\dagger(\pm\mathbf{k}) \rightarrow \alpha_\pm^\dagger(\pm\mathbf{k})e^{i\Lambda_\pm(\pm\mathbf{k})}$, and $P^\dagger(\mathbf{k}) \rightarrow P^\dagger(\mathbf{k})e^{i\Lambda(\mathbf{k})}$ in which $\Lambda(\mathbf{k}) = \Lambda_+(\mathbf{k}) + \Lambda_-(-\mathbf{k})$. Consequently, $\phi(\mathbf{k})$ and $\mathbf{A}_p(\mathbf{k})$ transform as $\phi(\mathbf{k}) \rightarrow \phi(\mathbf{k}) - \Lambda(\mathbf{k})$, and $\mathbf{A}_p(\mathbf{k}) \rightarrow \mathbf{A}_p(\mathbf{k}) - \nabla_{\mathbf{k}}\Lambda(\mathbf{k})$. We define a gauge invariant tangential vector field, “velocity”, on S_+ as $\mathbf{v}(\mathbf{k}) = \nabla_{\mathbf{k}}\phi(\mathbf{k}) - \mathbf{A}_p$, which is regular except at gap nodes. If we consider the case that $\Delta(\mathbf{k})$ only has isolated zeros located at \mathbf{k}_i ($i = 1, 2, \dots, n$). An infinitesimal oriented loop C_i is defined around each zero \mathbf{k}_i whose positive direction depends on the local normal direction by the right-hand rule. Then, $\oint_{C_i} d\mathbf{k} \cdot \mathbf{v} = 2\pi g_i$ in which g_i is the vorticity and integer-valued. Next, reversing the direction of each loop C_i and applying Stokes’ theorem on S_+ (excluding the bad points \mathbf{k}_i ’s on which \mathbf{v} is ill-defined), we arrive at

$$\sum_i g_i = \frac{1}{2\pi} \sum_i \oint_{C_i} d\mathbf{k} \cdot \mathbf{v} = \iint \frac{d\mathbf{k}}{2\pi} \cdot (\nabla_{\mathbf{k}} \times \mathbf{A}_p) = 2q_p. \quad (1)$$

This proof is gauge-independent. If $\Delta(\mathbf{k})$ has line-nodes on S_+ which behave as branch-cuts of \mathbf{v} , the proof can also be done similarly. \square

Remark. When $q_p \neq 0$, $\Delta(\mathbf{k})$ cannot be a regular function over the entire S_+ . Its nodal structure is distinct from that of the usual pairings characterized by spherical harmonics $Y_{lm}(\hat{\mathbf{k}})$, which are regular functions over the sphere. The absence of the monopole structure gives rise to vanishing total vorticity of phases. For example, for the $^3\text{He-A}$ type pairing with the orbital symmetry $Y_{11}(\hat{\mathbf{k}})$, two gap nodes lie at the north and south poles as a pair

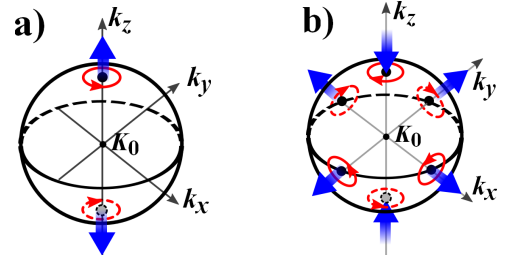


FIG. 1. The vorticity and nodal structure of the pairing gap function $\Delta(\mathbf{k})$ on the bulk Fermi surface S_+ . The total vorticities equal +2 according to Theorem 1. The vortices at the north and south poles exhibit the vorticity ± 1 for (a) $\Delta_y = -i\Delta_x$ and (b) $\Delta_y = i\Delta_x$, respectively. Each of the four additional nodes in (b) exhibit the vorticity +1.

of vortex and anti-vortex of the pairing phase field, respectively.

To illustrate this, we use a concrete simple model for the 3D Weyl metal defined in a bipartite array of lattice planes with spinless fermions^{34,42}.

$$H_K = \sum_{a,b} \sum_{\mathbf{k}} c_a^\dagger(\mathbf{k}) \left\{ [t_- \cos(2k_x) + t_+(k_y, k_z)] \sigma_x + \sin(2k_x) \sigma_y + V(k_y) \sigma_z - \mu I \right\} c_b(\mathbf{k}) + h.c., \quad (2)$$

in which the σ_z -eigenbasis refer to A and B sublattices; $V_{k_y} = 2k_y$, $t_+(k_y, k_z) = -(k_y^2 + k_z^2)$ and $t_- = 1$. H_K is invariant under the inversion transformation with respect to the center of a bond along x -direction, *i.e.*, $A \leftrightarrow B$, $k_{y,z} \rightarrow -k_{y,z}$, and it breaks TR symmetry, because the “spinless” fermions can be considered as fully-spin-polarized. It also has a mirror symmetry $k_z \rightarrow -k_z$, and has a pair of Weyl points at $\pm \mathbf{K}_0 = (0, 0, \pm 1)$ on the k_z -axis. If $\mu > 0$, the Fermi surface sheets FS_\pm enclosing $\pm \mathbf{K}_0$ have Chern numbers $C = \pm 1$, respectively. For small values of μ , FS_\pm are approximately spherical.

Consider the following pairing Hamiltonian

$$H_\Delta(\mathbf{k}) = \sum_{a,b} \sum_{\mathbf{k}} c_a^\dagger(\mathbf{k}) [2i\Delta_x \sin(2k_x) I + 2i\Delta_y \sin k_y \sigma_1]_{ab} c_b^\dagger(-\mathbf{k}) + h.c. \quad (3)$$

The constructions of Eqs. (2) and (3) on the lattice are presented in the Supplemental Material (Suppl. Mat.) A. Assuming that the system is in the weak pairing region, *i.e.*, $|\Delta_{x,y}| \ll |\mu|$, we can project the pairing onto FS_\pm . Since the gap function satisfies $\Delta(-\mathbf{k}) = -\Delta(\mathbf{k})$, we only need to consider $\Delta(\mathbf{k})$ on FS_+ . $\Delta(\mathbf{k})$ exhibits two nodes at the north and the south poles. We choose two different gauges, which are non-singular in the two polar regions. Then, the gap function can be approximated as $\Delta(\mathbf{k}) = \mp \Delta_x k_x + \Delta_y k_y$ at north and south poles, respectively. If $\Delta_y = -i\Delta_x$, the velocity field $\mathbf{v}(\mathbf{k})$ exhibits a pair of vortices located at north and south poles with the vorticity +1 (Fig. 1 (a)). There are no other nodes on FS_+ , and the total vorticity is +2 in agreement with

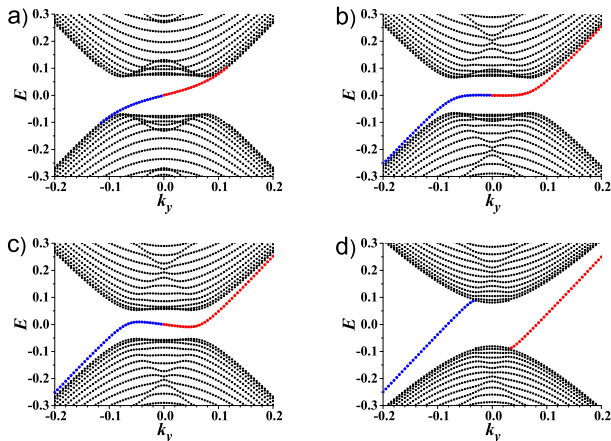


FIG. 2. (Color Online) The projected bulk and surface mode spectrum on a single open boundary of the yz -plane vs. k_y at different cuts of $k_z = 1.03, 0.95, 0.93, 0.85$ from (a) to (d), respectively. The parameters are $\Delta_y = -i\Delta_x$ with $\Delta_x = 0.2$ and $\mu = 0.2$. The cuts of k_z lie between the intersecting points of the z -axis on FS_+ for (a), (b), and (c), while k_z in (d) lies outside FS_+ . The red (blue) color represents the positive (negative) charge carried by the surface modes.

Theorem 1. In contrast, if $\Delta_y = i\Delta_x$, each of the nodes at the north and south poles changes its vorticity to -1 . To maintain the total vorticity, four additional nodes appear on FS_+ , each of which has vorticity $+1$ (Fig. 1 (b)). In our model, these four nodes are located on the equator with azimuthal angles $\pm\frac{\pi}{4}, \pm\frac{3\pi}{4}$.

We also calculated the surface spectra on the open boundary. In the absence of pairing, this model shows chiral surface states for k_z lying in the region $-K_{0,z} < k_z < K_{0,z}$ ⁴². Now, Cooper pairing opens pairing gaps on FS_\pm , and generates additional Majorana surface modes inside the pairing gaps. These Majorana surface modes are determined by the pairing nodal structure on FS_\pm and the associated vorticity pattern. As have been described in Ref. [52], these must connect to the Fermi arcs arising from the Weyl band structures as k_z varies.

We impose two open boundaries parallel to the yz -plane, and plot the spectra vs. k_y for different k_z , with modes localized on the bottom boundary suppressed. The results of the case $\Delta_y = -i\Delta_x$ are shown in Fig. 2 (a)-(d). Under the Bogoliubov-de Gennes (BdG) formalism, there are four quasiparticle bands, but only states with $k_z > 0$ are independent. Because of the mirror symmetry, the spectrum is invariant under $k_z \mapsto -k_z$ plus a particle-hole transformation. At $\mu = 0.2$, FS_+ enclosing $K_0 = (0, 0, 1)$ intersects the k_z -axis at $k_n \approx 1.1$ (the north pole) and $k_s \approx 0.9$ (the south pole). For the cut of $k_z > k_n$, or, $k_z < k_s$, it does not intersect FS_+ . The corresponding surface spectra are determined by the Weyl band structure: No surface modes exist at $k_z > k_n$, and two branches of chiral surface modes appear at $-k_s < k_z < k_s$ (Fig. 2 (d)). They are related by particle-hole transformation under which $(k_y, k_z) \mapsto$

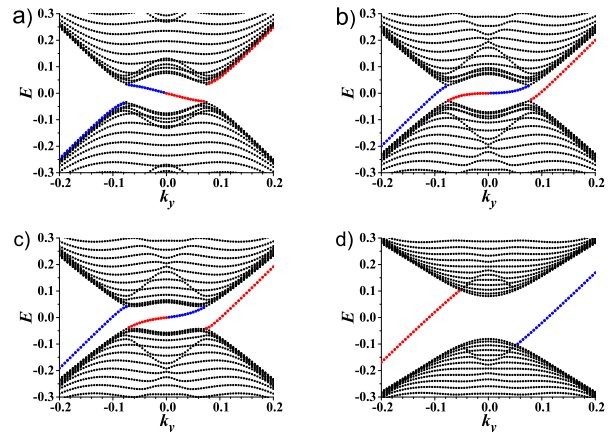


FIG. 3. (Color Online) The bulk and surface spectrum as in Fig. 2, except that $\Delta_y = i\Delta_x$ here. The chiralities of the Majorana surface modes at k_z close to the north and south poles are opposite to those in the case of $\Delta_y = -i\Delta_x$. (A topological change occurs at $k_z = 1.0$, between (a) and (b).)

$(-k_y, -k_z)$, which reverses their charge, followed by z -reflection, $(-k_y, -k_z) \mapsto (-k_y, k_z)$. Consequently, for fixed $-k_s < k_z < k_s$ one surface mode is entirely electron-like (the standard Fermi arc) with a quasiparticle charge $0 < e^*(k_y, k_z) < e$, and the other is the z -reflection of its particle-hole conjugate, with $e^*(-k_y, k_z) < 0$. Because k_z lies outside FS_\pm , the particle-hole mixing is weak, so the charge of the electron-line arc mode is close to e .

The change in surface band topology between $k_z > k_n$ and $-k_s < k_z < k_s$ must occur through gap closings at $k_z = k_n$ and k_s . In this region, each k_z defines a Fermi-surface cross section (“Fermi-CS”) on FS_+ of the Weyl metal, which becomes gapped by pairing. The only surviving bulk zero-energy excitations at the nodal points are Weyl-Majorana (WM) points in the BdG formalism, and classified as positive or negative according to their chiral indices. The two WM points at the north and south poles both carry positive pairing vorticities $+1$. As k_z decreases through the WM point at the north pole, the surface gap closes and reopens with a single surface mode passing through zero energy, as shown in Fig. 2(a-c). After k_z passes the WM point at the south pole, which also has pairing vorticity $+1$, the number of the branches of surface modes is increased to 2, as in the normal Weyl metal.

When $k_n > k_z > k_s$, the surface quasiparticle charge changes continuously as a function of k_y from hole-like to particle-like at a “neutrality point”, which in our model is pinned at $k_y = 0$ by the z -reflection symmetry $e^*(k_y, k_z) \equiv -e^*(-k_y, -k_z) = e^*(-k_y, k_z)$. In general, these points are on a “neutrality line” in the surface BZ connecting the projections of the two WM points. The z -reflection symmetry also gives the quasiparticle spectrum the symmetry $E(k_y, k_z) \equiv -E(-k_y, -k_z) = E(-k_y, k_z)$, so the zero-energy line, like the neutrality point is pinned to $k_y = 0$, and its group velocity is in the y direction. Near the

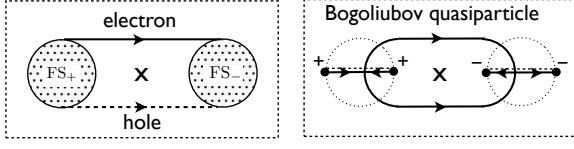


FIG. 4. (Schematic.) Zero-energy surface states in the surface Brillouin zone, with a chiral pair of projected bulk Fermi surfaces (left) or four projected bulk gapless superconductor nodes (right); “X” marks $\mathbf{k} = 0$. The directions on arcs are $\hat{\mathbf{n}} \times \hat{\mathbf{v}}$, where $\hat{\mathbf{n}}$ is the normal to the surface, and \mathbf{v} is the group velocity of the surface mode. The “flow”^{42,52} starts and ends at projections of sources and sinks of 3D Berry flux at the Fermi level. Right: a “vector central charge” $\tilde{c}\hat{\mathbf{v}}$ with $\tilde{c} = \frac{1}{2}$ is associated with the Bogoliubov edge modes (directed solid lines), with $\sum \tilde{c}\hat{\mathbf{v}} = 0$ at the “cross”, which is a special feature⁵² of mirror symmetry. Also shown (dashed line connecting nodes) is the quasiparticle “neutrality line”, which is only pinned to zero energy by the mirror symmetry.

north pole, the zero-energy point has group-velocity in the $+\hat{\mathbf{y}}$ direction, while near the south pole, it is along $-\hat{\mathbf{y}}$. A consequence of the reflection symmetry is that at some intermediate k_z , its group velocity vanishes, and for fixed k_z less than this, there are three values of k_y with a zero-energy quasiparticle, one electron-like, one hole-like, and one neutral. At this inflection point, the locus of zero-energy lines in the surface BZ has a “cross shape”⁵² (see Fig.4), that is a symmetry-protected feature of the z -reflection symmetry.

The surface spectra at the case of $\Delta_y = i\Delta_x$ were also calculated (Fig.3). The surface modes in the cases of $k_z > k_n$ and $k_s > k_z > 0$ are not directly related to pairing, and thus are qualitatively the same as the case of $\Delta_y = -i\Delta_x$. However, the Majorana surface modes at $k_n > k_z > k_s$ are markedly different due to the more complicated nodal structure on FS_+ . As shown in Fig.1(b), the WM points at the north and the south poles are negative; while those near the equator are positive. As k_z is reduced below k_n , a Majorana surface mode appears inside the pairing gap as in Fig.3(a), with opposite chirality to that in Fig.2(a). The gap closes again at $k_z = 1$, where projections of the four positive WM points are found. When the gap reopens, there are three modes with positive chirality, the neutral one of which disappears when the gap closes at the now-negative projected WM point at $k_z = k_s$.

Next we study the pairing partial-wave symmetries when FS_\pm have approximate spherical symmetry. If we neglect the small anisotropy, the complete bases of $\Delta(\mathbf{k})$ for \mathbf{k} lying on S_+ with the total vorticity q_p can be spanned by the monopole harmonic functions $Y_{q_p, j m}(\hat{\mathbf{k}})$ instead of the usual $Y_{l m}$. Monopole harmonic functions have been widely applied in physics^{4,56,57}. For completeness, their basic properties are summarized in Suppl. Mat. B. After projecting the pairing Hamiltonian to FS_\pm , it becomes $H_\Delta = \sum_{\mathbf{k}} \Delta(\mathbf{k}) P^\dagger(\mathbf{k}) + \Delta^*(\mathbf{k}) P(\mathbf{k})$ for \mathbf{k} lying close to S_+ . We define $\Delta(\mathbf{k}) = \Delta(|k|) f(\hat{\mathbf{k}})$, in

which the angular dependence on $\hat{\mathbf{k}}$ and the energy dependence on $|k|$ are separated. $\Delta(|k|)$ is assumed positive and the angular factor $f(\hat{\mathbf{k}})$ is complex satisfying the normalization condition $\int d\hat{\mathbf{k}} |f(\hat{\mathbf{k}})|^2 = 1$. $f(\hat{\mathbf{k}})$ is expanded in terms of the monopole harmonic functions as

$$f(\hat{\mathbf{k}}) = \sum_{j m} c_{j m} \mathcal{Y}_{q_p, j m}(\hat{\mathbf{k}}), \quad (4)$$

in which $c_{j m}$ are complex coefficients. Both the pairing operator $P^\dagger(\mathbf{k})$ and the gap function $\Delta(\mathbf{k})$ are gauge dependent, while, H_Δ is gauge independent.

A remarkable feature is that all the pairing channels should have $j \geq |q_p|$ regardless of the pairing mechanism since $\mathcal{Y}_{q_p, j, m}$ starts with $j = |q_p|$. The absence of pairing channels with $j < |q_p|$ is robust, as a consequence of topology and the monopole harmonic representation of the rotation group. Furthermore, the lowest order pairing channel $j = |q_p|$ is special: $\mathcal{Y}_{q_p, j=|q_p|, m}(\hat{\mathbf{k}})$ are holomorphic or anti-holomorphic functions. All of its $2q_p$ -nodes exhibit the same vorticity, and thus $\Delta(\mathbf{k})$ is completely determined by the locations of its nodes up to an overall factor. The nodes of $\mathcal{Y}_{q_p, j=|q_p|, m}(\hat{\mathbf{k}})$ represent vortices of the pairing phases on S_+ . The location of pairing nodes are also WM points of the BdG Hamiltonian with the same chirality. For each node on FS_+ with $\mathbf{K}_0 + \mathbf{k}$, there exists its image on FS_- exhibiting the opposite vorticity.

Let us consider a concrete example of spin-1/2 fermions in the continuum with spin-orbit coupling. The low energy kinetic Hamiltonians around the Weyl points are

$$H_{\text{Weyl}, \pm}(\pm \mathbf{K}_0 + \mathbf{k}) = \pm v_F \boldsymbol{\sigma} \cdot \mathbf{k} - \mu, \quad (5)$$

where σ 's represent Pauli matrices for spins; $\mu > 0$ is assumed without loss of generality. We choose the gauge convention: $\xi_+(\hat{\mathbf{k}}) = \xi_-(-\hat{\mathbf{k}}) = (u_{\hat{\mathbf{k}}}, v_{\hat{\mathbf{k}}})^T$, in which $u_{\hat{\mathbf{k}}} = \cos \frac{\theta_{\hat{\mathbf{k}}}}{2}$ and $v_{\hat{\mathbf{k}}} = \sin \frac{\theta_{\hat{\mathbf{k}}}}{2} e^{i\phi_{\hat{\mathbf{k}}}}$, which are singular when $\hat{\mathbf{k}}$ is located at the north and the south poles on FS_\pm , respectively. $P^\dagger(\mathbf{k}) = \alpha_+^\dagger(\mathbf{k}) \alpha_-^\dagger(-\mathbf{k})$ is a spin-1 helicity eigen-operator, satisfying $[\mathbf{S} \cdot \hat{\mathbf{k}}, P^\dagger(\mathbf{k})] = P^\dagger(\mathbf{k})$, in which \mathbf{S} is the total spin of the Cooper pair. Under the S_z -eigenbasis, $P^\dagger(\mathbf{k}) = \sum_{m=-1}^1 \sqrt{\frac{4\pi}{3}} \mathcal{Y}_{-1, 1 m}^*(\hat{\mathbf{k}}) \chi_{1 m}^\dagger(\mathbf{k})$, in which $\chi_{1 m}^\dagger(\mathbf{k}) = \langle 1 m | \frac{1}{2} \sigma \frac{1}{2} \sigma^\dagger c_\sigma^\dagger(\mathbf{K}_0 + \mathbf{k}) c_{\sigma'}^\dagger(-\mathbf{K}_0 - \mathbf{k})$. The monopole charge enclosed by S_+ is $q_p = -1$ for the phase distribution of $\Delta(\mathbf{k})$. According to Eq. (4), by setting $j = |q_p| = 1$, $f(\hat{\mathbf{k}})$ is a quadratic homogeneous function of u_k and v_k^* , $f(\hat{\mathbf{k}}) = f(u_k, v_k) = \frac{1}{\sqrt{N}} \prod_{i=1,2} (u_k v_i^* - u_i v_k^*)$, where N is the normalization factor; the nodal points are represented by $(u_i, v_i)^T = (\cos \frac{\theta_i}{2}, \sin \frac{\theta_i}{2} e^{i\phi_i})^T$ with $i = 1, 2$.

The locations of nodes in $f(\hat{\mathbf{k}})$ are determined by the energetics. The Ginzburg-Landau (GL) analysis (see Suppl. Mat. C.) shows that there are two typical possibilities for $j = 1$ that m in Eq. (4) equals 0, or ± 1 : In the former case,

$$\Delta_{m=0}(\mathbf{k}) = \Delta(|k|) \sin \theta_k e^{i\phi_k}. \quad (6)$$

In contrast to the usual case where $\Delta(\mathbf{k}) \propto Y_{10}(\hat{\mathbf{k}})$ exhibits a nodal line, Eq. (6) only has nodal points that repel each other, at antipodal points on S_+ . In realistic systems, the spherical symmetry of S_+ is broken down to a lower point-group symmetry. Since the pairing gap is suppressed around gap nodes, the gap nodes may preferentially locate at the minima of local density of states on S_+ . In the lattice case, two nodes attract each other and merge into a double one. Without loss of generality, they can locate at the north or south pole as

$$\Delta(\mathbf{k}) = \begin{cases} \Delta(|k|) \cos^2 \frac{\theta_k}{2} & (m = 1), \\ \Delta(|k|) \sin^2 \frac{\theta_k}{2} e^{2i\phi_k} & (m = -1), \end{cases} \quad (7)$$

respectively. Again, its nodal structure is distinct from the usual axial pairing with orbital symmetry characterized by spherical harmonic function $\mathcal{Y}_{1\pm 1}(\hat{\mathbf{k}})$. The pairing structures of Eq. (6) and Eq. (7) in the representation of σ_z -basis have also been studied in the context of pairing with magnetic dipolar interactions⁵⁸.

The monopole Cooper-pairing described above can be generalized to Fermi surfaces carrying opposite Chern numbers $\pm C$ with $C \geq 2$. In these cases, the monopole charge enclosed by the pairing surface S_+ equals $q_p = C$. The mean-field free energy favors single nodes, and nodes repel each other forming a vortex lattice configuration, although optimal configurations may be complicated by energetic issues.

We have also performed the partial-wave analysis of the pairing interactions (see Suppl. Mat. D) to show how the non-trivial topology of FS_{\pm} transforms the ordinary partial-wave channels into those characterized by

monopole harmonics starting with $j = |q_p|$. Another possibility of Cooper pairing in doped Weyl metals is intra-Fermi surface pairing with non-zero center of mass momenta, whose pairing phase structure does not possess non-trivial Berry phase structure on FS_{\pm} (see Suppl. Mat. E.).

In summary, we have studied the Cooper pairing structure between two separate Fermi surfaces carrying opposite Chern numbers $\pm C$. The Cooper pairs carry a non-trivial Berry phase structure characterized by the monopole charge $q_p = C$ so that their phases cannot be globally well-defined on the Fermi surfaces. The gap function $\Delta(\mathbf{k})$ generically possesses nodes with the total vorticity $2q_p$. These nodes are also the WM points of the Hamiltonian in the BdG formalism. The surface modes arise both from the Weyl band structure and the pairing: the former exist inside the band gap, while the latter appear inside the pairing gap on FS_{\pm} . In a simplified model where FS_{\pm} are both spherical, the pairing symmetry is classified in terms of the monopole harmonic functions. The lowest pairing channel is $j = |q_p|$ purely determined by the symmetry rather than interaction, and the corresponding pairing functions are holomorphic or anti-holomorphic functions on the pairing surface.

Acknowledgments Y.L. thanks the Princeton Center for Theoretical Science at Princeton University for support. F.D.M.H. was supported in part by the MRSEC program at Princeton Center for Complex Materials, grant NSF-DMR-1420541, and by the W. M. Keck Foundation.

-
- ¹ K. v. Klitzing, G. Dorda, and M. Pepper, Phys. Rev. Lett. **45**, 494 (1980).
² D. C. Tsui, H. L. Stormer, and A. C. Gossard, Phys. Rev. Lett. **48**, 1559 (1982).
³ D. J. Thouless, M. Kohmoto, M. P. Nightingale, and M. den Nijs, Phys. Rev. Lett. **49**, 405 (1982).
⁴ F. Haldane, Phys. Rev. Lett. **51**, 605 (1983).
⁵ J. E. Avron, R. Seiler, and B. Simon, Phys. Rev. Lett. **51**, 51 (1983).
⁶ Q. Niu, D. Thouless, and Y. Wu, Phys. Rev. B **31**, 3372 (1985).
⁷ M. Kohmoto, Ann. Phys. **160**, 343 (1985).
⁸ J. E. Avron, R. Seiler, and B. Simon, Phys. Rev. Lett. **65**, 2185 (1990).
⁹ F. D. M. Haldane, Phys. Rev. Lett. **61**, 2015 (1988).
¹⁰ R. Karplus and J. M. Luttinger, Phys. Rev. **95**, 1154 (1954).
¹¹ T. Jungwirth, Q. Niu, and A. H. MacDonald, Phys. Rev. Lett. **88**, 207208 (2002).
¹² M. Onoda and N. Nagaosa, J. Phys. Soc. Jpn. **71**, 19 (2002).
¹³ F. D. M. Haldane, Phys. Rev. Lett. **93**, 206602 (2004).
¹⁴ N. Nagaosa, J. Sinova, S. Onoda, A. H. MacDonald, and N. P. Ong, Rev. Mod. Phys. **82**, 1539 (2010).
¹⁵ R. Yu, W. Zhang, H.-J. Zhang, S.-C. Zhang, X. Dai, and Z. Fang, Science **329**, 61 (2010).
¹⁶ C.-Z. Chang, J. Zhang, X. Feng, J. Shen, Z. Zhang, M. Guo, K. Li, Y. Ou, P. Wei, L.-L. Wang, Z.-Q. Ji, Y. Feng, S. Ji, X. Chen, J. Jia, X. Dai, Z. Fang, S.-C. Zhang, K. He, Y. Wang, L. Lu, X.-C. Ma, and Q.-K. Xue, Science **340**, 167 (2013).
¹⁷ C. L. Kane and E. J. Mele, Phys. Rev. Lett. **95**, 226801 (2005).
¹⁸ C. L. Kane and E. J. Mele, Phys. Rev. Lett. **95**, 146802 (2005).
¹⁹ B. A. Bernevig and S.-C. Zhang, Phys. Rev. Lett. **96**, 106802 (2006).
²⁰ B. A. Bernevig, T. L. Hughes, and S.-C. Zhang, Science **314**, 1757 (2006).
²¹ L. Fu and C. L. Kane, Phys. Rev. B **76**, 045302 (2007).
²² L. Fu, C. L. Kane, and E. J. Mele, Phys. Rev. Lett. **98**, 106803 (2007).
²³ J. E. Moore and L. Balents, Phys. Rev. B **75**, 121306 (2007).
²⁴ X.-L. Qi, T. L. Hughes, and S.-C. Zhang, Phys. Rev. B **78**, 195424 (2008).
²⁵ R. Roy, Phys. Rev. B **79**, 195322 (2009).
²⁶ M. Z. Hasan and C. L. Kane, Rev. Mod. Phys. **82**, 3045 (2010).
²⁷ X.-L. Qi and S.-C. Zhang,

- Rev. Mod. Phys. **83**, 1057 (2011).
- ²⁸ X. Wan, A. M. Turner, A. Vishwanath, and S. Y. Savrasov, Phys. Rev. B **83**, 205101 (2011).
- ²⁹ A. A. Burkov and L. Balents, Phys. Rev. Lett. **107**, 127205 (2011).
- ³⁰ K.-Y. Yang, Y.-M. Lu, and Y. Ran, Phys. Rev. B **84**, 075129 (2011).
- ³¹ T. Meng and L. Balents, Phys. Rev. B **86**, 054504 (2012).
- ³² W. Witczak-Krempa and Y. B. Kim, Phys. Rev. B **85**, 045124 (2012).
- ³³ G. Y. Cho, J. H. Bardarson, Y.-M. Lu, and J. E. Moore, Phys. Rev. B **86**, 214514 (2012).
- ³⁴ P. Hosur, Phys. Rev. B **86**, 195102 (2012).
- ³⁵ C. Fang, M. J. Gilbert, X. Dai, and B. A. Bernevig, Phys. Rev. Lett. **108**, 266802 (2012).
- ³⁶ D. T. Son and B. Z. Spivak, Phys. Rev. B **88**, 104412 (2013).
- ³⁷ P. Hosur and X. Qi, Comptes Rendus Physique **14**, 857 (2013), arXiv:1309.4464 [cond-mat.str-el].
- ³⁸ M. M. Vazifeh and M. Franz, Phys. Rev. Lett. **111**, 027201 (2013).
- ³⁹ R. Nandkishore, D. A. Huse, and S. L. Sondhi, Phys. Rev. B **89**, 245110 (2014).
- ⁴⁰ P. Hosur, X. Dai, Z. Fang, and X.-L. Qi, Phys. Rev. B **90**, 045130 (2014).
- ⁴¹ A. C. Potter, I. Kimchi, and A. Vishwanath, Nat. Commun. **5**, 5161 (2014).
- ⁴² F. D. M. Haldane, ArXiv e-prints (2014), arXiv:1401.0529 [cond-mat.str-el].
- ⁴³ H. Wei, S.-P. Chao, and V. Aji, Phys. Rev. B **89**, 014506 (2014).
- ⁴⁴ H. Weng, C. Fang, Z. Fang, B. A. Bernevig, and X. Dai, Phys. Rev. X **5**, 011029 (2015).
- ⁴⁵ A. A. Burkov, J. Phys.: Condens. Matter **27**, 113201 (2015).
- ⁴⁶ S.-Y. Xu, I. Belopolski, N. Alidoust, M. Neupane, G. Bian, C. Zhang, R. Sankar, G. Chang, Z. Yuan, C.-C. Lee, S.-M. Huang, H. Zheng, J. Ma, D. S. Sanchez, B. Wang, A. Bansil, F. Chou, P. P. Shibayev, H. Lin, S. Jia, and M. Z. Hasan, Science **349**, 613 (2015).
- ⁴⁷ S.-Y. Xu, N. Alidoust, I. Belopolski, Z. Yuan, G. Bian, T.-R. Chang, H. Zheng, V. N. Strocov, D. S. Sanchez, G. Chang, *et al.*, Nature Phys. **11**, 748754 (2015).
- ⁴⁸ B. Q. Lv, H. M. Weng, B. B. Fu, X. P. Wang, H. Miao, J. Ma, P. Richard, X. C. Huang, L. X. Zhao, G. F. Chen, Z. Fang, X. Dai, T. Qian, and H. Ding, Phys. Rev. X **5**, 031013 (2015).
- ⁴⁹ B. Q. Lv, N. Xu, H. M. Weng, J. Z. Ma, P. Richard, X. C. Huang, L. X. Zhao, G. F. Chen, C. Matt, F. Bisti, V. Strocov, J. Mesot, Z. Fang, X. Dai, T. Qian, M. Shi, and H. Ding, Nature Phys. , 724 (2015).
- ⁵⁰ G. Bednik, A. A. Zyuzin, and A. A. Burkov, ArXiv e-prints (2015), arXiv:1506.05109 [cond-mat.str-el].
- ⁵¹ S.-K. Jian, Y.-F. Jiang, and H. Yao, Phys. Rev. Lett. **114**, 237001 (2015).
- ⁵² B. Lu, K. Yada, M. Sato, and Y. Tanaka, Phys. Rev. Lett. **114**, 096804 (2015).
- ⁵³ S. Borisenko, D. Evtushinsky, Q. Gibson, A. Yaresko, T. Kim, M. Ali, B. Buechner, M. Hoesch, and R. J. Cava, 392 (2015), arXiv:1507.04847.
- ⁵⁴ Y. Qi, P. G. Naumov, M. N. Ali, C. R. Rajamathi, O. Barkalov, Y. Sun, C. Shekhar, S.-C. Wu, V. Süß, M. Schmidt, E. Pippel, P. Werner, R. Hillebrand, T. Förster, E. Kampertt, W. Schnelle, S. Parkin, R. J. Cava, C. Felser, B. Yan, and S. A. Medvedev, ArXiv e-prints (2015), arXiv:1508.03502 [cond-mat.mtrl-sci].
- ⁵⁵ J. Xiong, S. K. Kushwaha, T. Liang, J. W. Krizan, W. Wang, R. J. Cava, and N. P. Ong, ArXiv e-prints: 1503.08179 (2015), arXiv:1503.08179 [cond-mat.str-el].
- ⁵⁶ T. T. Wu and C. N. Yang, Nucl. Phys. B **107**, 365 (1976).
- ⁵⁷ T. T. Wu and C. N. Yang, Phys. Rev. D **16**, 1018 (1977).
- ⁵⁸ Y. Li and C. Wu, Scientific Reports **2**, 392 (2012).
- ⁵⁹ A. Larkin and Y. N. Ovchinnikov, Zh. Eksperim. i Teor. Fiz. **47** (1964).
- ⁶⁰ P. Fulde and R. A. Ferrell, Phys. Rev. **135**, A550 (1964).
- ⁶¹ X.-L. Qi, T. L. Hughes, and S.-C. Zhang, Phys. Rev. B **81**, 134508 (2010).

Supplemental Materials

A. Lattice construction of the Weyl metal model

The Weyl metal model Eq. (2) studied in the main text can be formulated in the real space in a bipartite lattice with spinless fermions⁴². After a partial Fourier transformation over the y and z -directions, the band Hamiltonian along the x -axis becomes

$$H_{k_y, k_z}^K = V_{k_y} \sum_i \left\{ c_{k_y, k_z}^{A, \dagger}(i) c_{k_y, k_z}^A(i) - c_{k_y, k_z}^{B, \dagger}(i) c_{k_y, k_z}^B(i) \right\} + \sum_i \left\{ t_+(k_y, k_z) c_{k_y, k_z}^{B, \dagger}(i) c_{k_y, k_z}^A(i+1) + t_- c_{k_y, k_z}^{A, \dagger}(i) c_{k_y, k_z}^B(i) + h.c. \right\}, \quad (8)$$

in which i is the index of unit cells containing A and B sites, $V_{k_y} = 2k_y$, $t_+(k_y, k_z) = -(k_y^2 + k_z^2)$ and $t_- = 1$. H^K is invariant under the inversion transformation with respect to the center of a bond along x -direction, *i.e.*, $A \leftrightarrow B$, $k_{y,z} \rightarrow -k_{y,z}$, and it breaks TR symmetry. This Hamiltonian gives rise to a pair of Weyl point located at $\pm \mathbf{K}_0 = (0, 0, \pm 1)$, respectively. For chemical potential $\mu > 0$, FS $_{\pm}$ enclosing $\pm \mathbf{K}_0$ possess the Chern number $C = \pm 1$, respectively. Consider the following pairing structure

$$H_{k_y, k_z}^{\Delta} = \sum_{i, a=A, B} \left\{ \Delta_x c_{k_y, k_z}^{a, \dagger}(i) c_{-k_y, -k_z}^a(i+1) + h.c. \right\} + \sum_i \left\{ 2i \Delta_y \sin k_y c_{k_y, k_z}^{A, \dagger}(i) c_{-k_y, -k_z}^B(i) + h.c. \right\}. \quad (9)$$

After projection to FS $_{+}$, the gap function $\Delta(\mathbf{k})$ exhibits two nodes at the north and south poles, respectively.

B. Monopole harmonic functions

In this section, we present the definition and basic properties of monopole harmonic functions. For convenience, we will formulate mostly in real space, and their momentum version can be obtained by replacing $\hat{\mathbf{r}}$ with $\hat{\mathbf{k}}$.

Consider a magnetic monopole located at the origin. For convenience, we choose the following gauge to describe its vector potential \mathbf{A} as

$$\mathbf{A}(\mathbf{r}) = \frac{g}{r} \frac{\hat{\mathbf{z}} \times \mathbf{r}}{|\mathbf{r}| + \mathbf{r} \cdot \hat{\mathbf{z}}} = \frac{g}{r} \tan \frac{\theta}{2} \hat{\phi}, \quad (10)$$

which is singular along the Dirac string from the origin to the south pole. The mechanical angular momentum is defined as $\mathbf{\Lambda} = \mathbf{r} \times (\mathbf{p} - \frac{e}{c} \mathbf{A})$, but $\mathbf{\Lambda}$ does not satisfy the commutation of the SU(2) algebra. The angular momentum satisfying the SU(2) algebra is define as

$$\mathbf{L} = \mathbf{\Lambda} - q \hat{\mathbf{r}}, \quad (11)$$

where $q = \frac{eg}{c\hbar}$. q is a positive integer, or, half-integer, taking values of $\frac{1}{2}, 1, \frac{3}{2}, 2, \dots$. Because $\mathbf{\Lambda} \perp \mathbf{r}$, we can verify that

$$\Lambda^2 = L^2 - \hbar^2 q^2, \quad (12)$$

which is an operator identity. If an electron is confined on a sphere with radius R with a monopole of charge q located in the center of the sphere, its Hamiltonian can be described as

$$H = \frac{\hbar^2}{2mR^2} \Lambda^2 \quad (13)$$

The components of $L_{\pm} = L_x \pm iL_y$ and L_z are

$$L_z = -i\hbar \frac{\partial}{\partial \phi} - \hbar q$$

$$L_{\pm} = \hbar e^{\pm i\phi} \left(\pm \frac{\partial}{\partial \theta} + i \cot \theta \frac{\partial}{\partial \phi} - q \tan \frac{\theta}{2} \right), \quad (14)$$

L^2 is expressed as

$$\frac{L^2}{\hbar^2} = \frac{-1}{\sin^2 \theta} (\sin \theta \frac{\partial}{\partial \theta} (\sin \theta \frac{\partial}{\partial \theta} + \frac{1}{\sin^2 \theta} (i \frac{\partial}{\partial \phi} + q(1 - \cos \theta))^2 + \hbar^2 q^2). \quad (15)$$

The monopole harmonic functions $\mathcal{Y}_{q;jj_z}(\theta, \phi)$ are defined as

$$L^2 \mathcal{Y}_{q;jj_z}(\theta, \phi) = j(j+1) \hbar^2 \mathcal{Y}_{q;jj_z}(\theta, \phi)$$

$$L_z \mathcal{Y}_{q;jj_z}(\theta, \phi) = j_z \hbar \mathcal{Y}_{q;jj_z}(\theta, \phi), \quad (16)$$

where $j = |q|, |q| + 1, \dots$, and $j_z = -j, -j + 1, \dots, j$. There is a nice relation between the monopole harmonic functions and the rotation D -matrix as

$$\mathcal{Y}_{q;jm}(\theta, \phi) = \sqrt{\frac{2j+1}{4\pi}} \left[D_{m, -q}^j(\phi, \theta, -\phi) \right]^*$$

$$= \sqrt{\frac{2j+1}{4\pi}} e^{i(m+q)\phi} d_{m, -q}^j(\theta) \quad (17)$$

where $D_{m, m'}^j(\alpha, \beta, \gamma)$ is defined in the standard way as

$$D_{m, m'}^j(\alpha, \beta, \gamma) = \langle jm | e^{-iJ_z \alpha} e^{-iJ_y \beta} e^{-iJ_z \gamma} | jm' \rangle$$

$$= e^{-im\alpha - im'\gamma} d_{m, m'}^j(\beta), \quad (18)$$

and $d_{m, m'}^j(\beta) = \langle jm | e^{-iJ_y \beta} | jm' \rangle$. The expression for $d_{m, m'}^j(\beta)$ is

$$d_{m, m'}^j(\beta) = \sqrt{\frac{(j+m')!(j-m)!}{(j+m)!(j-m)!}} \left(\cos \frac{\beta}{2} \right)^{m'+m}$$

$$\times \left(\sin \frac{\beta}{2} \right)^{m'-m} P_{j-m'}^{m'-m, m'+m}(\cos \beta), \quad (19)$$

where the Jacobi polynomial $P_{j-m'}^{m'-m, m'+m}(\cos \beta)$ follows the definition as

$$P_n^{a, b}(x) = \frac{(-)^n}{2^n n!} (1-x)^{-a} (1+x)^{-b}$$

$$\times \frac{d^n}{dx^n} [(1-x)^{a+n} (1+x)^{b+n}]. \quad (20)$$

It will also be useful to introduce the two-component spinor notation $u = \cos \frac{\theta}{2}, v = \sin \frac{\theta}{2} e^{i\phi}$. In this notation, the expression of $\mathcal{Y}_{-q;j=q,j_z}(\theta, \phi)$ is simple in which $q > 0$ as

$$\mathcal{Y}_{-q;j=q,m}(\theta, \phi) = \left\{ \frac{2q+1}{4\pi} \binom{2q}{q-m} \right\}^{\frac{1}{2}} u^{q+m} v^{*,q-m}. \quad (21)$$

The relation between $\mathcal{Y}_{q;jm}(\theta, \phi)$ and $\mathcal{Y}_{-q;jm}(\theta, \phi)$ is

$$\mathcal{Y}_{q;jm}(\theta, \phi) = (-)^{q+m} \mathcal{Y}_{-q;j-m}^*(\theta, \phi).$$

For the purpose of the main body article, we will use monopole harmonic functions defined in momentum space. To maintain the SU(2) algebra, the angular momentum operator \mathbf{L} in the presence of the monopole is augmented to

$$\mathbf{L} = \hbar \mathbf{k} \times \left(-i\partial_{\mathbf{k}} - \frac{1}{k} \mathbf{A}(\mathbf{k}) \right) - q\hbar \hat{\mathbf{k}}, \quad (22)$$

and the vector potential under the gauge chosen above is $\mathbf{A}(\mathbf{k}) = q \tan \frac{\theta_{\mathbf{k}}}{2} \hat{e}_{\phi_{\mathbf{k}}}$. We can simply replace polar and azimuthal angles of θ and ϕ of \hat{r} with that of \hat{q} in the expressions above to yield $\mathcal{Y}_{q;jm}(\hat{\mathbf{k}})$. Again for $\mathcal{Y}_{q;jm}(\hat{\mathbf{k}})$, j starts with $|q|$ and takes values of $|q|, |q| + 1, \dots$. For the lowest value $j = |q|$, $\mathcal{Y}_{q;j=|q|,m}(\hat{\mathbf{k}})$'s are holomorphic (anti-holomorphic) functions on the unit sphere for $q < 0$ ($q > 0$).

C. Ginzburg-Landau analysis

To analyze the possible pairing configuration with $j = |q_p| = 1$, we perform the GL free energy analysis. The GL free energy is constructed as

$$F_G = \alpha |\Delta|^2 + \beta_1 |\Delta|^4 + \beta_2 |\Delta|^4 \sum_{mm'} c_{1m}^* c_{1,-m}^* c_{1m'} c_{1,-m'},$$

in which $|\Delta|$ is the magnitude of gap and the normalized coefficients c_{1m} defined in Eq. (4) control the angular distribution of the gap function. Without loss of generality, F_{GL} is minimized when c_{1m} 's take the component of $m = 1$ or $m = -1$ at $\beta_2 > 0$ and of $m = 0$ at $\beta_2 < 0$, respectively. Applying rotations to these configurations generates other equivalent pairing configurations. Following the standard terminology, we denote the former cases of $m = \pm 1$ and the latter one of $m = 0$ as the axial and the polar pairing, respectively.

The Bogoliubov quasi-particle spectra become

$$E(\mathbf{k}) = \sqrt{\epsilon_k^2 + \Delta^2 (|k|) |f(u_k, v_k)|^2}. \quad (23)$$

Assuming a fixed magnitude $\Delta(|k|)$ and normalized $f(\hat{\mathbf{k}})$, the free energy functional depends on the location of nodes through the relation of $F[u_k, v_k] = -\frac{2}{\beta} \sum_{\mathbf{k}} \ln(2 \cosh \beta E(\mathbf{k}))$. Different from the vortex problem in real space, $F[u_k, v_k]$ does not depend on the phase

gradient in momentum space but only on the magnitude distribution of $\Delta(\mathbf{k})$. Because of the convexity of F , the two nodes repel each other on S_+ , and in the optimal configuration they lie at two ends of a diameter, say, the north and south poles. In other words, the mean-field results give rise to $\beta_2 < 0$, and the corresponding pairing is polar with $m = 0$. Nevertheless, that case of $\beta_2 > 0$ cannot be ruled out. The consequential axial pairing with $m = \pm 1$ will result beyond the mean-field theory arising from strong correlation effect.

D. Partial-wave analysis of interactions by monopole harmonics

In this section, we elaborate the pair scattering interactions. Since the inter-Fermi surface Cooper pairing is between two electrons with parallel spins for the FS $_{\pm}$, we only consider the triplet channel pairing whose Hamiltonian is expressed as

$$H_{pair} = \frac{1}{V_0} \sum_{\mathbf{k}, \mathbf{k}'; m} V_t(\mathbf{k}, \mathbf{k}') \chi_{1m}^\dagger(\mathbf{k}) \chi_{1m}(\mathbf{k}') + h.c., \quad (24)$$

in which V_0 is the system volume; $\chi_{1m}^\dagger(\mathbf{k}) = \sum_{\sigma\sigma'} \langle 1m | \frac{1}{2}\sigma; \frac{1}{2}\sigma' \rangle c_\sigma^\dagger(\mathbf{K}_0 + \mathbf{k}) c_{\sigma'}^\dagger(-\mathbf{K}_0 - \mathbf{k})$ are the spin triplet pairing operator. Because usual interactions in solids do not directly flip electron spins, the spin index m in Eq. (24) is expressed in the S_z -eigenbasis. Eq. (24) is not expressed in the helical basis, and hence it is still not the low energy pairing Hamiltonian in accommodation to the helical Fermi surfaces yet. After projecting the pairing Hamiltonian Eq. (24) into the helical Fermi surface, we arrive at

$$\tilde{H}_{pair} = \sum_{\mathbf{k}, \mathbf{k}'} \tilde{V}(\mathbf{k}, \mathbf{k}') P^\dagger(\mathbf{k}) P(\mathbf{k}') + h.c., \quad (25)$$

in which $\tilde{V}(\mathbf{k}, \mathbf{k}') = \langle P(\mathbf{k}') | H_{pair} | P(\mathbf{k}) \rangle$ is the projected pair scattering matrix element. It can be expressed as

$$\tilde{V}(\mathbf{k}, \mathbf{k}') = \frac{4\pi}{3} \mathcal{Y}_{-1;1m}^*(\hat{\mathbf{k}}) V_t(\mathbf{k}, \mathbf{k}') \mathcal{Y}_{-1;1m}(\hat{\mathbf{k}}'). \quad (26)$$

Here, $P(\mathbf{k}) = \sum_{m=-1}^1 \sqrt{\frac{4\pi}{3}} \mathcal{Y}_{-1;1m}(\hat{\mathbf{k}}) \chi_{1m}(\mathbf{k})$ was used and the rotational invariance of the interaction was assumed. $\Delta(\mathbf{k})$ is the gap function determined by the self-consistent equation

$$\Delta(\mathbf{k}) = \frac{1}{V_0} \sum_{\mathbf{k}'} \tilde{V}(\mathbf{k}, \mathbf{k}') \langle P(\mathbf{k}') \rangle. \quad (27)$$

Because of fermion statistics, the pair scattering matrix element in Eq. (24) is expressed as

$$V_t(\mathbf{k}, \mathbf{k}') = V(\mathbf{k} - \mathbf{k}') - V(\mathbf{k} + \mathbf{k}' + 2\mathbf{K}_0), \quad (28)$$

in which the first and second terms are the intra and inter-Fermi surface scattering, respectively. If we neglect the inter-Fermi surface scattering which involves large

momentum transfer, $V_t(\mathbf{k}, \mathbf{k}')$ can be assumed only depending on the relative angle between \mathbf{k} and \mathbf{k}' , i.e., $V_t(\mathbf{k}, \mathbf{k}') = V_t(\hat{\mathbf{k}} \cdot \hat{\mathbf{k}}')$. Unlike the usual case, i.e., $\mathbf{K}_0 = 0$, that V_t only contains the odd partial-wave channels, here, both even and odd partial-wave channels are allowed as $V(\hat{\mathbf{k}} \cdot \hat{\mathbf{k}}') = \sum_{lm} 4\pi g_l Y_{lm}^*(\hat{\mathbf{k}}) Y_{lm}(\hat{\mathbf{k}})$ in which $l = 0, 1, 2, \dots$. As will be proved below, after the projection defined in Eq. (26), the pairing interaction becomes

$$\tilde{V}(\hat{\mathbf{k}} \cdot \hat{\mathbf{k}}') = \sum_{jm} \tilde{g}_j \mathcal{Y}_{-1, jm}^*(\hat{\mathbf{k}}) \mathcal{Y}_{1, jm}(\hat{\mathbf{k}}), \quad (29)$$

in which

$$\tilde{g}_j = \frac{1}{2j+1} \sum_{l=j, j\pm 1} (2l+1) g_l |\langle l0; 11 | j1 \rangle|^2, \quad (30)$$

and the partial wave channels start with $j = 1$. In other words, the projection to the helical Fermi surfaces reorganize the partial-wave channels, and thus promoted the lowest partial wave channel from $j = 0$ to $j = 1$. The actual pairing channel that the system takes is determined by the most negative pairing matrix eigenvalue $V_{j'}$.

Below, we prove Eq. (29). Starting from Eq. (26), since V_t can be decomposed by usual spherical harmonics, we have

$$\tilde{V}(\hat{\mathbf{k}} \cdot \hat{\mathbf{k}}') = -\frac{(4\pi)^2}{3} \sum_{m_1} \mathcal{Y}_{-1, 1m_1}^*(\hat{\mathbf{k}}) \mathcal{Y}_{-1, 1m_1}(\hat{\mathbf{k}}') \left[\sum_{l_2 m_2} g_{l_2} Y_{l_2 m_2}^*(\hat{\mathbf{k}}) Y_{l_2 m_2}(\hat{\mathbf{k}}') \right]. \quad (31)$$

where g_{l_2} is the interaction strength of V_t in the l_2 -th partial-wave channel. To further simplify $\tilde{V}(\hat{\mathbf{k}} \cdot \hat{\mathbf{k}}')$, the composition of monopole harmonics^{56,57} will be employed, which can be derived by using D-matrices as follows: Let us start from the composition known for irreducible tensors of angular momentum,

$$\Phi_{l_1 l_2 l_3 m_3} = \sum_{m_1 m_2} \Phi_{l_1 m_1} \Phi_{l_2 m_2} \langle l_3, m_3 | l_1, m_1; l_2, m_2 \rangle, \quad (32)$$

Alternatively,

$$\Phi_{l_1 m_1} \Phi_{l_2 m_2} = \sum_{l_3 m_3} \Phi_{l_1 l_2 l_3 m_3} \langle l_3, m_3 | l_1, m_1; l_2, m_2 \rangle \quad (33)$$

Applying a rotation to both sides of Eq. (33), we have

$$D(g) \Phi_{l_1 m_1} \Phi_{l_2 m_2} = \sum_{l_3 m_3} D(g) \Phi_{l_1 l_2 l_3 m_3} \langle l_3, m_3 | l_1, m_1; l_2, m_2 \rangle. \quad (34)$$

It can be represented by D-matrices as

$$\sum_{m'_1 m'_2} \Phi_{l_1 m'_1} \Phi_{l_2 m'_2} D_{m'_1, m_1}^{l_1}(g) D_{m'_2, m_2}^{l_2}(g) = \sum_{l_3 m_3 m'_3} \Phi_{l_1 l_2 l_3 m'_3} D_{m'_3, m_3}^{l_3}(g) \langle l_3, m_3 | l_1, m_1; l_2, m_2 \rangle, \quad (35)$$

Using Eq. (32), the right hand side of the above equation becomes

$$\sum_{l_3 m_3 m'_3} \sum_{m'_1 m'_2} \Phi_{l_1 m'_1} \Phi_{l_2 m'_2} D_{m'_3, m_3}^{l_3}(g) \langle l_3, m'_3 | l_1, m'_1; l_2, m'_2 \rangle \langle l_3, m_3 | l_1, m_1; l_2, m_2 \rangle. \quad (36)$$

Therefore, the composition rule of D-matrices is obtained as

$$D_{m'_1, m_1}^{l_1}(g) D_{m'_2, m_2}^{l_2}(g) = \sum_{l_3 m_3 m'_3} \langle l_3, m'_3 | l_1, m'_1; l_2, m'_2 \rangle \langle l_3, m_3 | l_1, m_1; l_2, m_2 \rangle D_{m'_3, m_3}^{l_3}(g). \quad (37)$$

By changing variables, we have

$$D_{m_1, -q_1}^{l_1*}(g) D_{m_2, -q_2}^{l_2*}(g) = \sum_{l_3 = |l_1 - l_2|}^{l_1 + l_2} \langle l_3, m_3 | l_1, m_1; l_2, m_2 \rangle \langle l_3, -q_3 | l_1, -q_1; l_2, -q_2 \rangle D_{m_3, -q_3}^{l_3*}(g), \quad (38)$$

where $m_3 = m_1 + m_2$, $q_3 = q_1 + q_2$. Using Eq. (17), the composition of monopole harmonics can be derived from the above composition of D-matrices as

$$\sqrt{\frac{4\pi}{2l_1+1}} \sqrt{\frac{4\pi}{2l_2+1}} \mathcal{Y}_{q_1; l_1 m_1}(\hat{\mathbf{k}}) \mathcal{Y}_{q_2; l_2 m_2}(\hat{\mathbf{k}}) = \sum_{l_3} \langle l_3, m_3 | l_1, m_1; l_2, m_2 \rangle \langle l_3, -q_3 | l_1, -q_1; l_2, -q_2 \rangle \sqrt{\frac{4\pi}{2l_3+1}} \mathcal{Y}_{q_3; l_3 m_3}(\hat{\mathbf{k}}). \quad (39)$$

For our derivation, let us take a special case of $q_1 = -1$, $q_2 = 0$, and $l_1 = 1$,

$$\mathcal{Y}_{-1;1m_1}(\hat{\mathbf{k}})Y_{l_2m_2}(\hat{\mathbf{k}}) = \sum_{l_3=l_2-1}^{l_2+1} \sqrt{\frac{3(2l_2+1)}{4\pi(2l_3+1)}} \langle l_3, m_3 | 1, m_1; l_2, m_2 \rangle \langle l_3, 1 | 1, 1; l_2, 0 \rangle \mathcal{Y}_{-1;l_3m_3}(\hat{\mathbf{k}}). \quad (40)$$

Then, Eq. (31) can be simplified as

$$\begin{aligned} \tilde{V}(\hat{\mathbf{k}} \cdot \hat{\mathbf{k}}') &= -4\pi \sum_{l_2} g_{l_2} \sum_{m_1, m_2} \sum_{l_3=l_2-1}^{l_2+1} \sum_{l'_3=l_2-1}^{l_2+1} \frac{2l_2+1}{\sqrt{(2l_3+1)(2l'_3+1)}} \times \\ &\quad \times \langle l_3, m_3 | 1, m_1; l_2, m_2 \rangle \langle l_3, 1 | 1, 1; l_2, 0 \rangle \mathcal{Y}_{-1;l_3m_3}^*(\hat{\mathbf{k}}) \times \\ &\quad \times \langle l'_3, m_3 | 1, m_1; l_2, m_2 \rangle \langle l'_3, 1 | 1, 1; l_2, 0 \rangle \mathcal{Y}_{-1;l'_3m_3}(\hat{\mathbf{k}}'). \end{aligned} \quad (41)$$

The orthogonality of Clebsch-Gordan coefficients $\sum_{m_2} \langle l_3, m_3 | 1, m_3 - m_2; l_2, m_2 \rangle \langle l'_3, m_3 | 1, m_3 - m_2; l_2, m_2 \rangle = \delta_{l_3l'_3}$ further gives

$$\begin{aligned} \tilde{V}(\hat{\mathbf{k}} \cdot \hat{\mathbf{k}}') &= -4\pi \sum_{l_2} g_{l_2} \sum_{l_3=l_2-1}^{l_2+1} \frac{2l_2+1}{2l_3+1} \langle l_3, 1 | 1, 1; l_2, 0 \rangle^2 \sum_{m_3} \mathcal{Y}_{-1;l_3m_3}^*(\hat{\mathbf{k}}) \mathcal{Y}_{-1;l_3m_3}(\hat{\mathbf{k}}') \\ &= -4\pi \sum_{l_3m_3} \tilde{g}_{l_3} \mathcal{Y}_{-1;l_3m_3}^*(\hat{\mathbf{k}}) \mathcal{Y}_{-1;l_3m_3}(\hat{\mathbf{k}}'). \end{aligned} \quad (42)$$

where $\tilde{g}_{l_3} = \frac{1}{2l_3+1} \sum_{l_2=l_3-1}^{l_3+1} (2l_2+1)g_{l_2} \langle l_3, 1 | 1, 1; l_2, 0 \rangle^2$ as shown in Eq. (29).

E. Intra-Fermi surface pairing

Another pairing possibility is the intra Fermi surface pairing: Cooper pairings take place within each Fermi surface FS_{\pm} carrying finite momentum $\pm \mathbf{K}_0$, respectively, thus this is an example of the Fulde-Ferrel-Larkin-Ovchinnikov type pairing^{59,60}. The intra FS_{\pm} pairing operators are defined as

$$P_+^{\dagger}(\mathbf{k}) = \alpha_+^{\dagger}(\mathbf{k})\alpha_+^{\dagger}(-\mathbf{k}), P_-^{\dagger}(\mathbf{k}) = \alpha_-^{\dagger}(\mathbf{k})\alpha_-^{\dagger}(-\mathbf{k}), \quad (43)$$

which satisfy $[\mathbf{S} \cdot \hat{\mathbf{k}}, P_{\pm}^{\dagger}(\mathbf{k})] = 0$. Therefore, their pairing phases can be well-defined globally over the sphere $|k| = k_f$ without non-trivial monopole structure, such that the gap functions can be decomposed into the usual spherical harmonic functions as $\Delta_{\pm}(\mathbf{k}) =$

$\Delta_{jm}(|k|) \sum_{j'm'} c_{\pm, j'm'} \mathcal{Y}_{j'm'}(\hat{\mathbf{k}})$. In the simplest case with $j = m = 0$, the pairing $\Delta_{0,\pm}$ is a mixture between the conventional s -wave and ${}^3\text{He-B}$ type p -wave pairings. Under the σ_z -eigen basis, they are written as

$$P_{\pm}(\mathbf{k}) \propto \chi_{\pm,00}^{\dagger}(\mathbf{k}) \pm \mathbf{k} \cdot \chi_{\pm}(\mathbf{k}), \quad (44)$$

in which the singlet and triplet pairing operators are $\chi_{\pm,00}^{\dagger}(\mathbf{k}) = \sum_{\alpha\beta} \langle 00 | \frac{1}{2}\alpha \frac{1}{2}\beta \rangle c_{\alpha}^{\dagger}(\pm \mathbf{K}_0 + \mathbf{k}) c_{\beta}^{\dagger}(\pm \mathbf{K}_0 - \mathbf{k})$, and $\chi_{\pm}(\mathbf{k}) = c_{\alpha}^{\dagger}(\pm \mathbf{K}_0 + \mathbf{k}) i(\sigma_y \sigma)_{\alpha\beta} c_{\beta}^{\dagger}(\pm \mathbf{K}_0 - \mathbf{k})$. This pairing is fully gapped, and thus can be characterized by the integer-valued topological index in the DIII class for 3D superconductivity. According to the criterion in Ref. [61], the overall pairing structure is topologically non-trivial according to $\Delta_+ = \mp \Delta_-$, respectively. The competition between the inter- and intra-Fermi surface pairing is an interesting question depending on the concrete pairing mechanism.